ESI

Enhanced gas separation performance of an ultramicroporous pillared-layer framework induced by hanging bare Lewis basic pyridine groups

Haipeng Li,[a] Shu'ni Li,*[a] Xiangyang Hou,[a,b] Yucheng Jiang,[a] Mancheng Hu,[a] Quan-Guo Zhai*[a]

[a] *Key Laboratory of Macromolecular Science of Shaanxi Province, Key Laboratory of Applied Surface and Colloid Chemistry, Ministry of Education, School of Chemistry & Chemical Engineering, Shaanxi Normal University, Xi'an, Shaanxi, 710062, P. R. China*

[b] *Department of Chemistry and Chemical Engineering, Yan'an University Laboratory of New Energy & New Function Materials, Yan'an Key Laboratory of Analytical Technology and Detection, Yan'an University, Shaanxi 716000, China*

**Corresponding authors,*

E-mail: lishuni@snnu.edu.cn; zhaiqg@snnu.edu.cn

Table S1. Crystal data and structure refinements for **SNNU-95**.

Compound	SNNU-95 (CCDC 1832498)
Empirical formula	$C_{44}H_{28}Co_2N_7O_7$
Formula weight	884.59
Crystal system	Monoclinic
Space group	*P*2(1)/*c*
a(Å)	11.3738(4)
b(Å)	29.4286(10)
c(Å)	17.1665(8)
α (deg)	90
β (deg)	99.870(4)
γ (deg)	90
Volume(Å^3)	5660.8(4)
Z	4
$d_{calcd.}$ (g·cm^{-3})	1.038
μ(mm^{-1})	0.629
F(000)	1804
Reflections collected/unique	26765 / 11562
R_{int}	0.0492
Data/restraints/parameters	11562 / 0 / 541
GOF on F^2	1.062
R_1[a], wR_2[b] [I > 2σ(I)]	0.0786, 0.2306
R_1[a], wR_2[b] (all data)	0.1011, 0.2473

[a] $R_1 = \Sigma||F_o|-|F_c||/\Sigma|F_o|$. [b] $wR_2 = [\Sigma w(F_o^2 - F_c^2)^2/\Sigma w(F_o^2)^2]^{1/2}$.

Table S2. Selected bond lengths (Å) and angles (°) for **SNNU-95**.

Co(1)-O(6)	2.048(3)	Co(2)-O(1)	2.144(4)
Co(1)-O(4) #1	2.075(3)	Co(2)-N(2) #3	2.150(3)
Co(1)-N(6) #2	2.085(4)	Co(2)-O(2)	2.188(4)
Co(1)-N(5)	2.144(3)	Co(2)-O(3) #1	2.015(4)
Co(1)-N(3) #3	2.169(3)	Co(2)-N(4)	2.137(3)
		Co(2)-O(5)	1.975(3)
N(5)-Co(1)-N(3)#3	177.38(14)	O(5)-Co(2)-O(1)	154.49(16)
O(5)-Co(2)-O(3)#1	100.20(15)	O(3)#1-Co(2)-O(1)	105.29(16)
O(5)-Co(2)-N(4)	92.35(15)	N(4)-Co(2)-O(1)	86.32(15)
O(3)#1-Co(2)-N(4)	90.53(14)	O(5)-Co(2)-N(2)#3	88.12(15)
N(6)#2-Co(1)-N(5)	93.76(15)	O(3)#1-Co(2)-N(2)#3	92.39(14)
O(6)-Co(1)-N(3)#3	91.82(13)	N(4)-Co(2)-N(2)#3	176.91(14)
O(4)#1-Co(1)-N(3)#3	89.37(13)	O(1)-Co(2)-N(2)#3	91.94(14)
N(6)#2-Co(1)-N(3)#3	88.84(14)	O(5)-Co(2)-O(2)	95.47(16)
O(6)-Co(1)-O(4)#1	163.70(14)	O(3)#1-Co(2)-O(2)	164.06(17)
O(6)-Co(1)-N(6)#2	96.43(15)	N(4)-Co(2)-O(2)	85.91(15)
O(4)#1-Co(1)-N(6)#2	99.84(14)	O(1)-Co(2)-O(2)	59.02(17)
O(6)-Co(1)-N(5)	87.63(14)	N(2)#3-Co(2)-O(2)	91.00(15)
O(4)#1-Co(1)-N(5)	90.44(13)		

Symmetry codes: #1 x,-y+1/2,z-1/2;#2 -x+1,y+1/2,-z+1/2 ; #3 x+1, y, z.

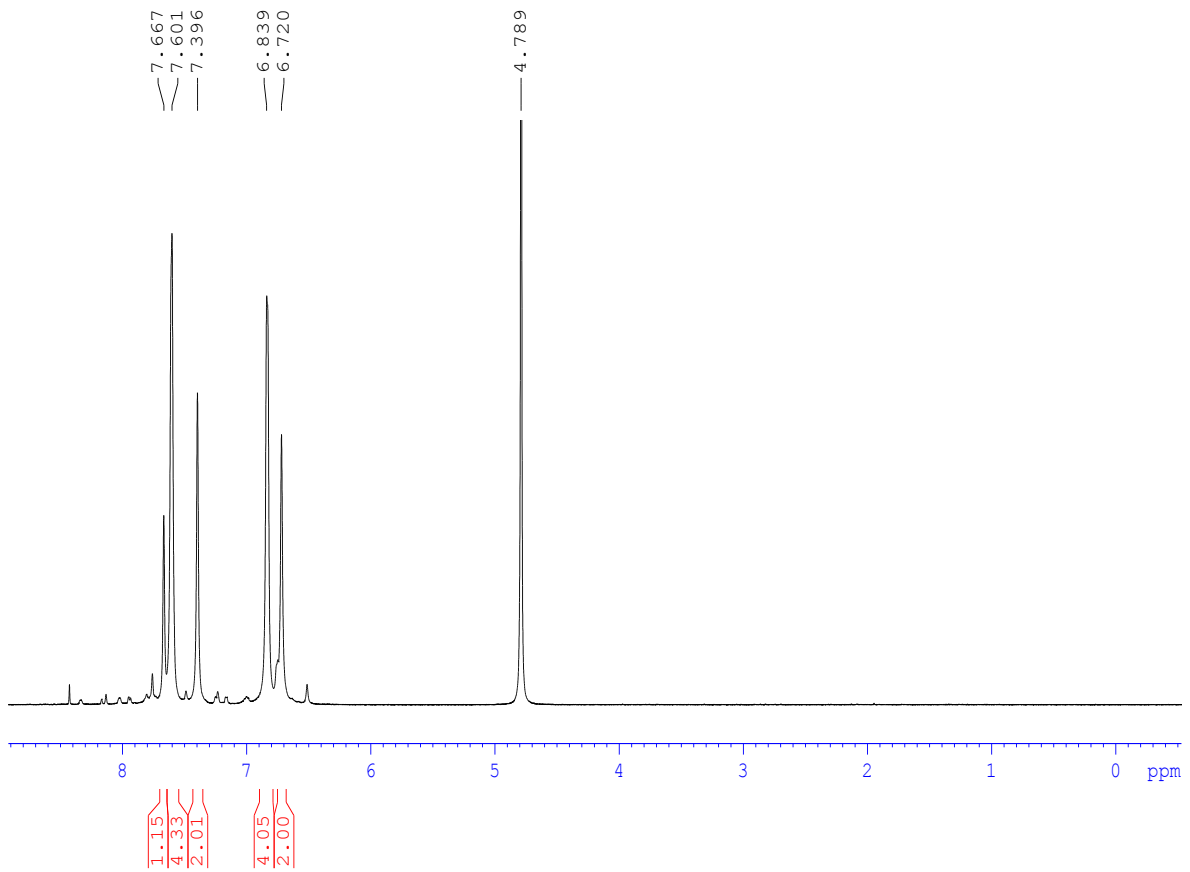

Fig. S1 The NMR spectrum of the synthesized H_2DBPT ligand. HNMR ($CDCl_3$, 400 MHz): 7.667 (s, 1H; H_{Ar}), 7.601(s, 4H; H_{Py}), 7.396(s, 2H; H_{Py}), 6.839(s, 4H; H_{Py}), 6.72 (s, 2H; H_{Ar}).

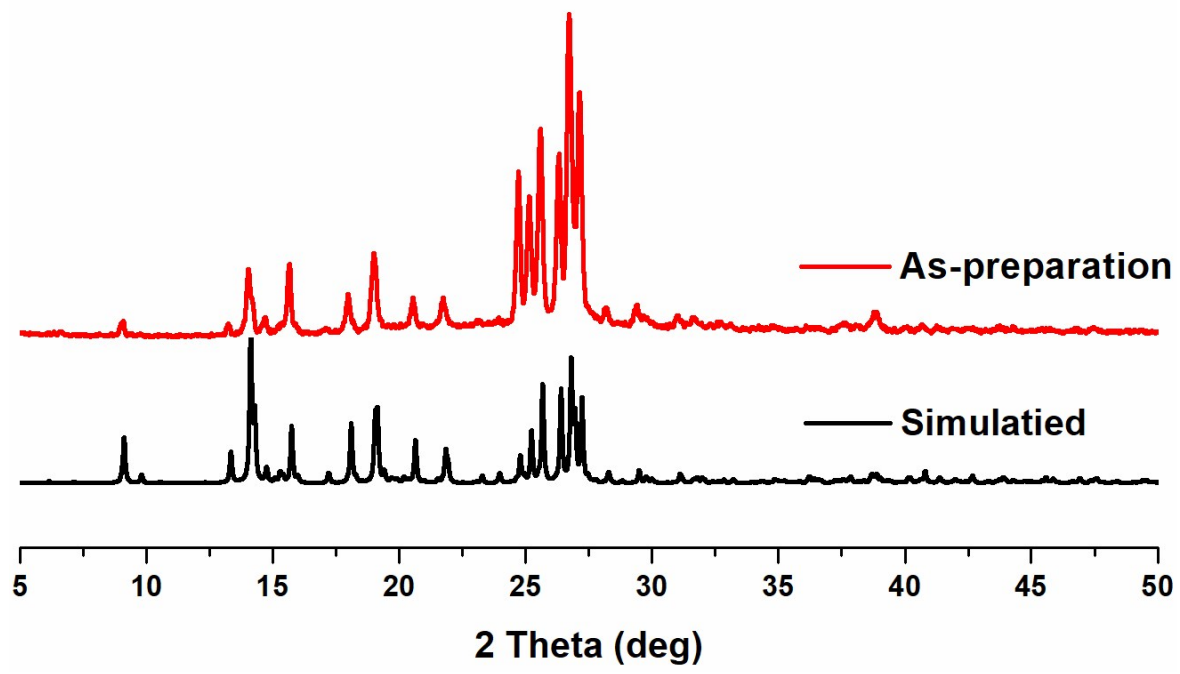

Fig. S2 PXRD patterns for the synthesized H_2DBPT ligand at room temperature.

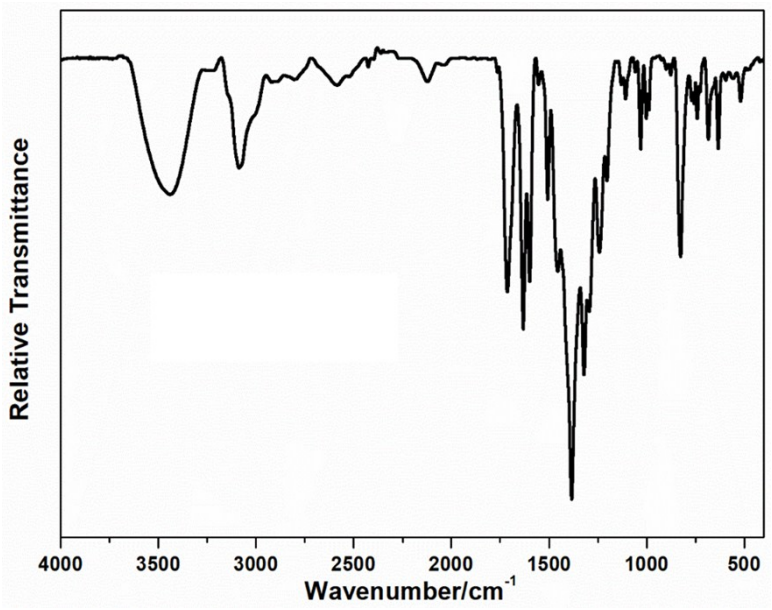

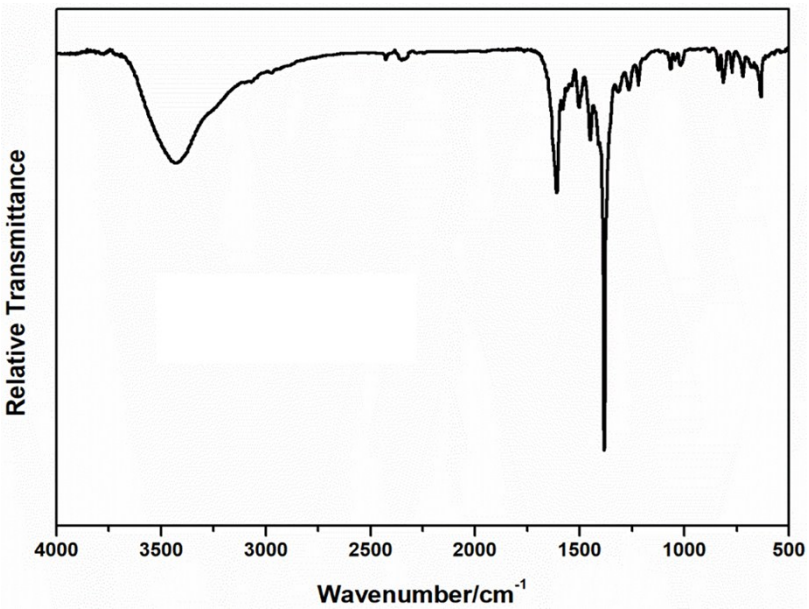

Fig. S3 FT-IR spectra for H_2DBPT (top) and **SNNU-95** (bottom).

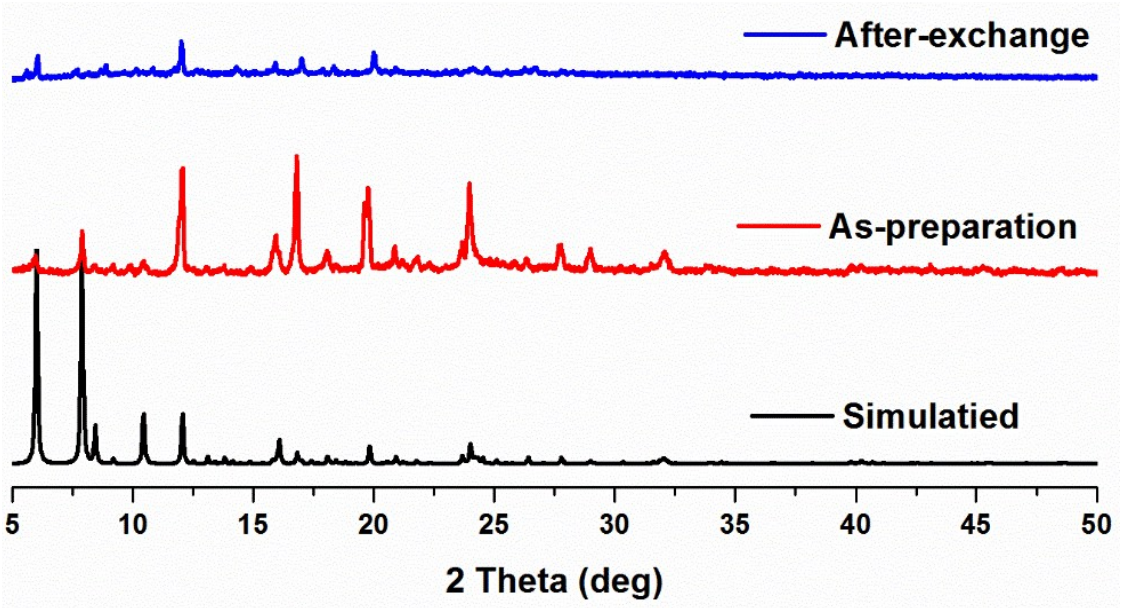

Fig. S4 PXRD patterns for **SNNU-95** at room temperature.

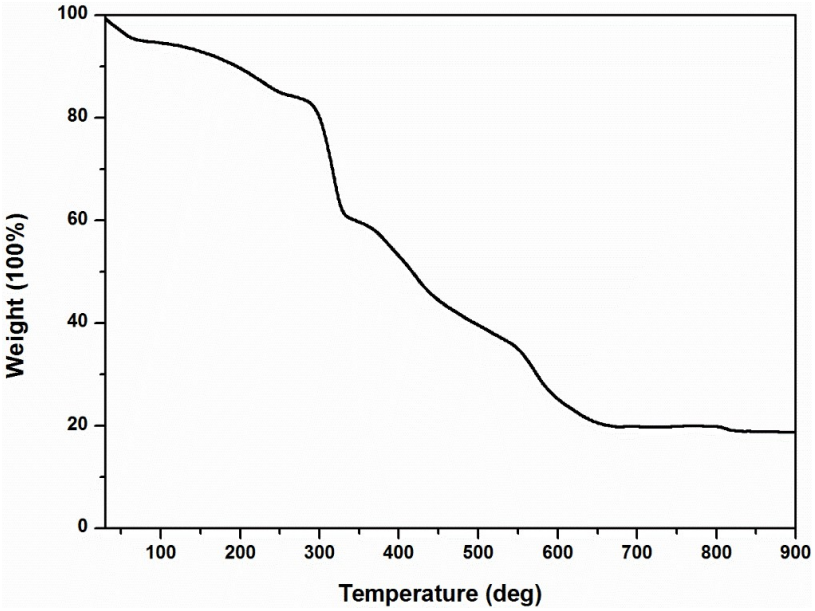

Fig. S5 TGA curve for **SNNU-95**.

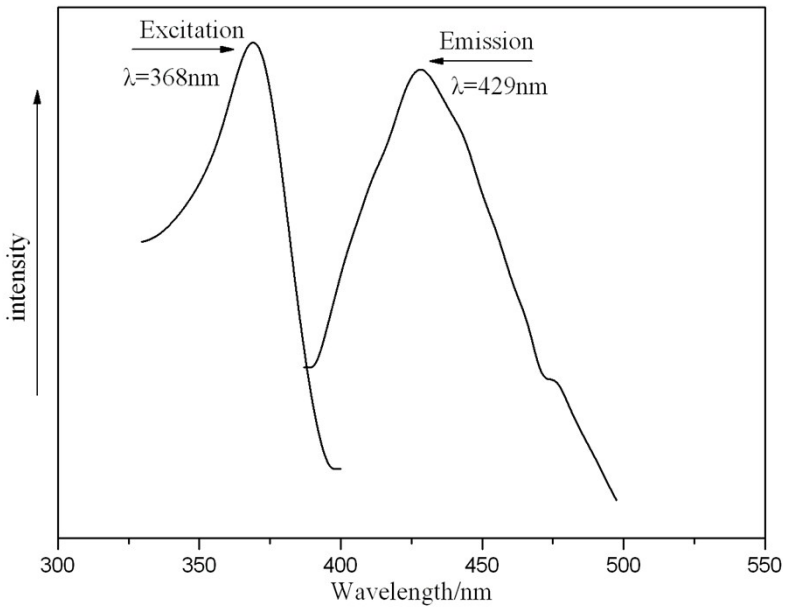

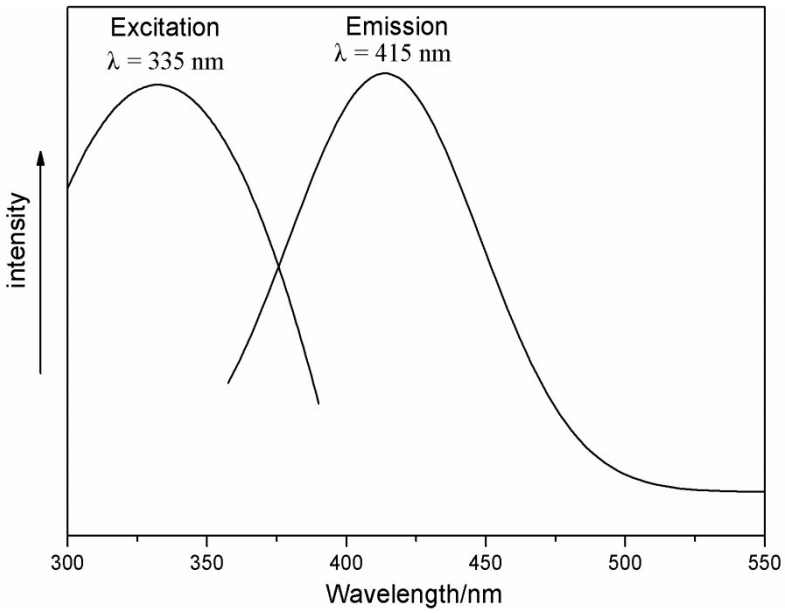

Fig. S6 The luminescent spectra of H_2DBPT (top) and **SNNU-95** (bottom) in solid state at room temperature.

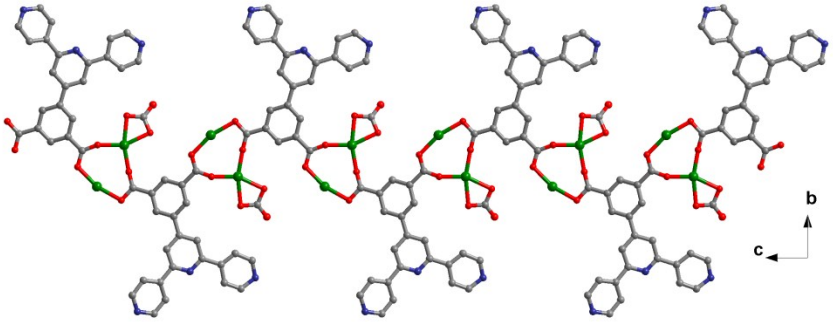

(a)

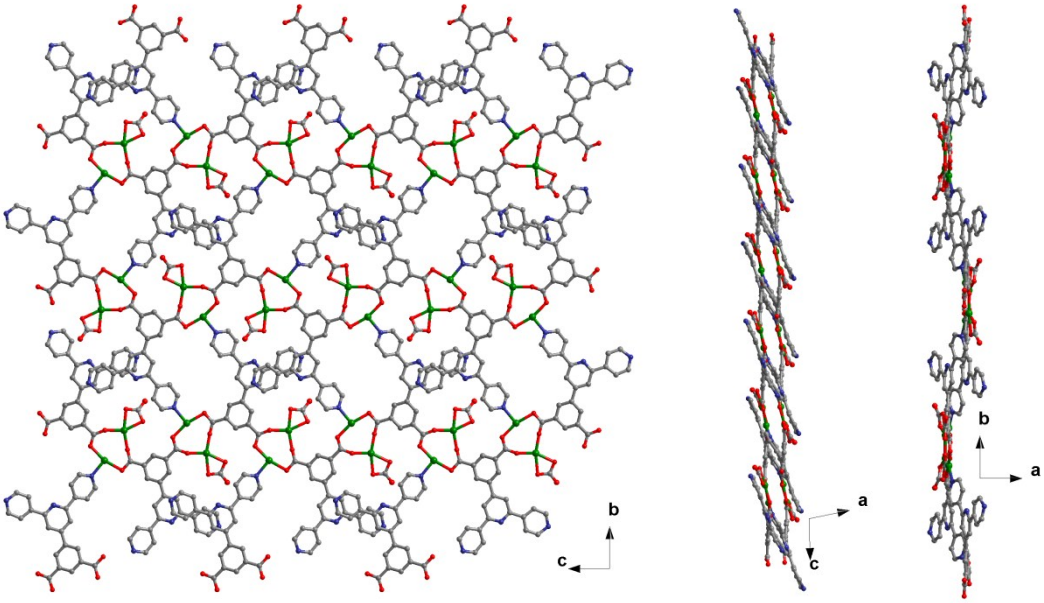

(b)

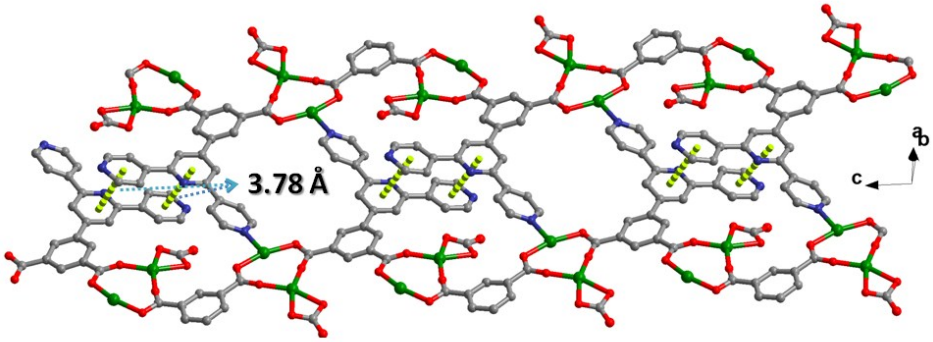

(c)

Fig. S7 1D chain generated by carboxylate groups from DBPT (a), 2D layer viewed from different directions (b), and the strong π···π stacking interactions within 2D layer in **SNNU-95**.

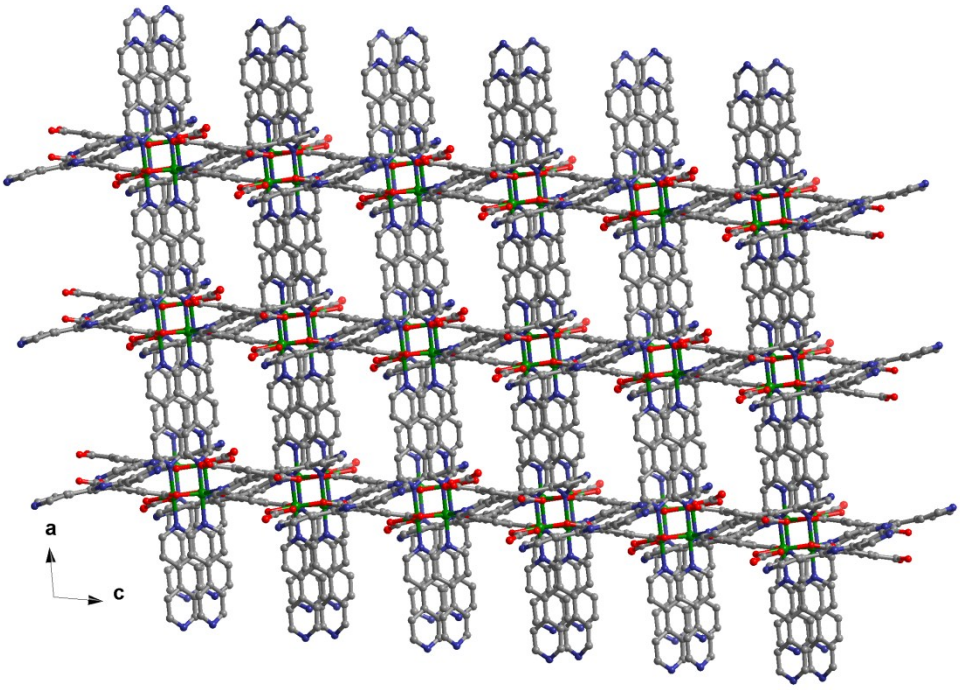

(a)

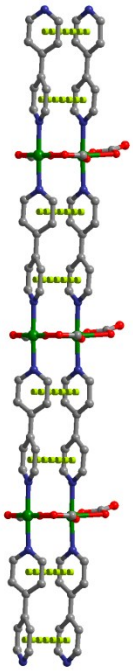

(b)

Fig. S8 3D pillared-layer framework viewed from b-axis direction (a) and strong π···π stacking interactions within pillars in **SNNU-95**.

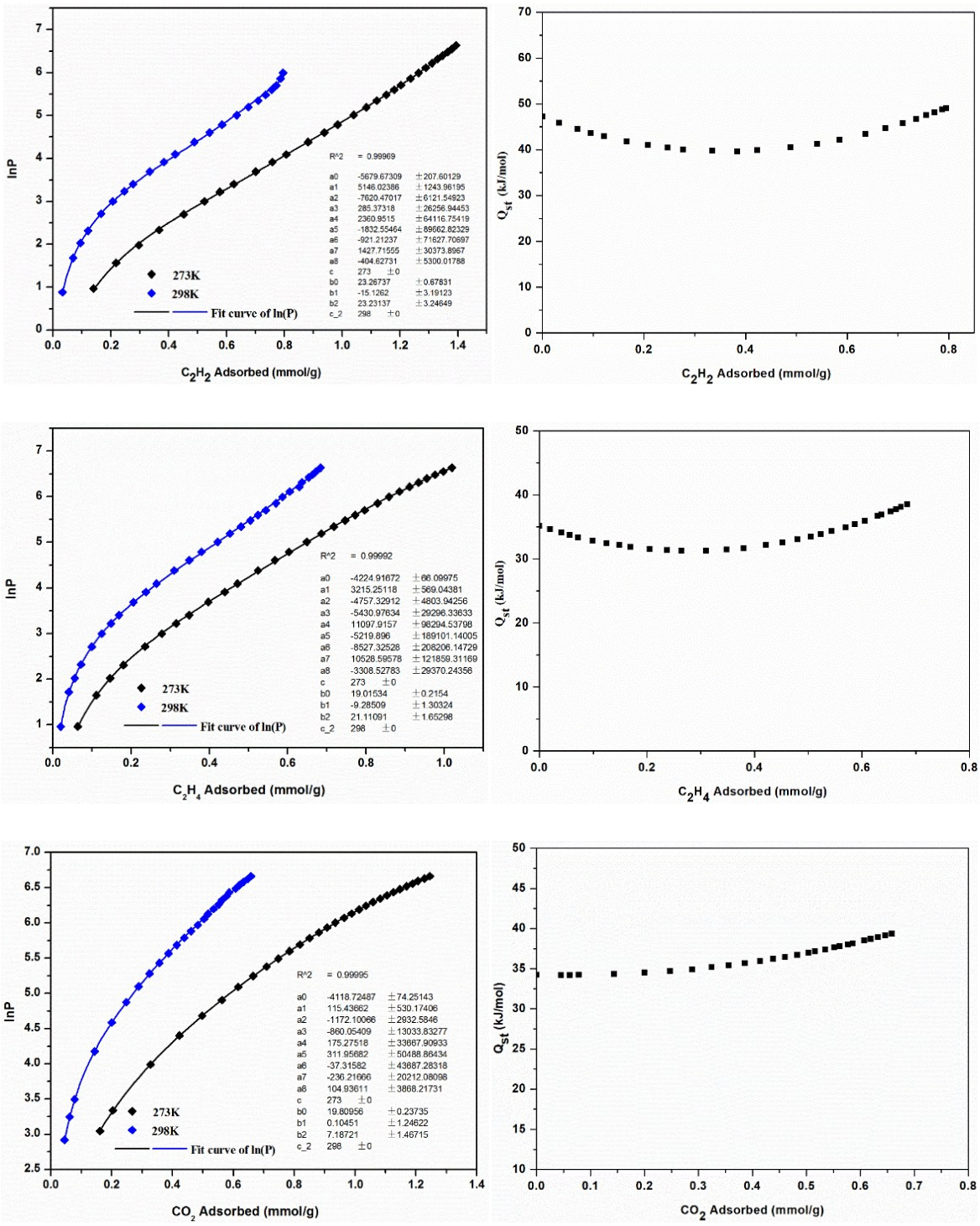

Fig. S9 Fitted gas adsorption isotherms of **SNNU-95** measured at 273 K and 298 K (left), and their corresponding isosteric heats of adsorption (Q_{st}) (right).

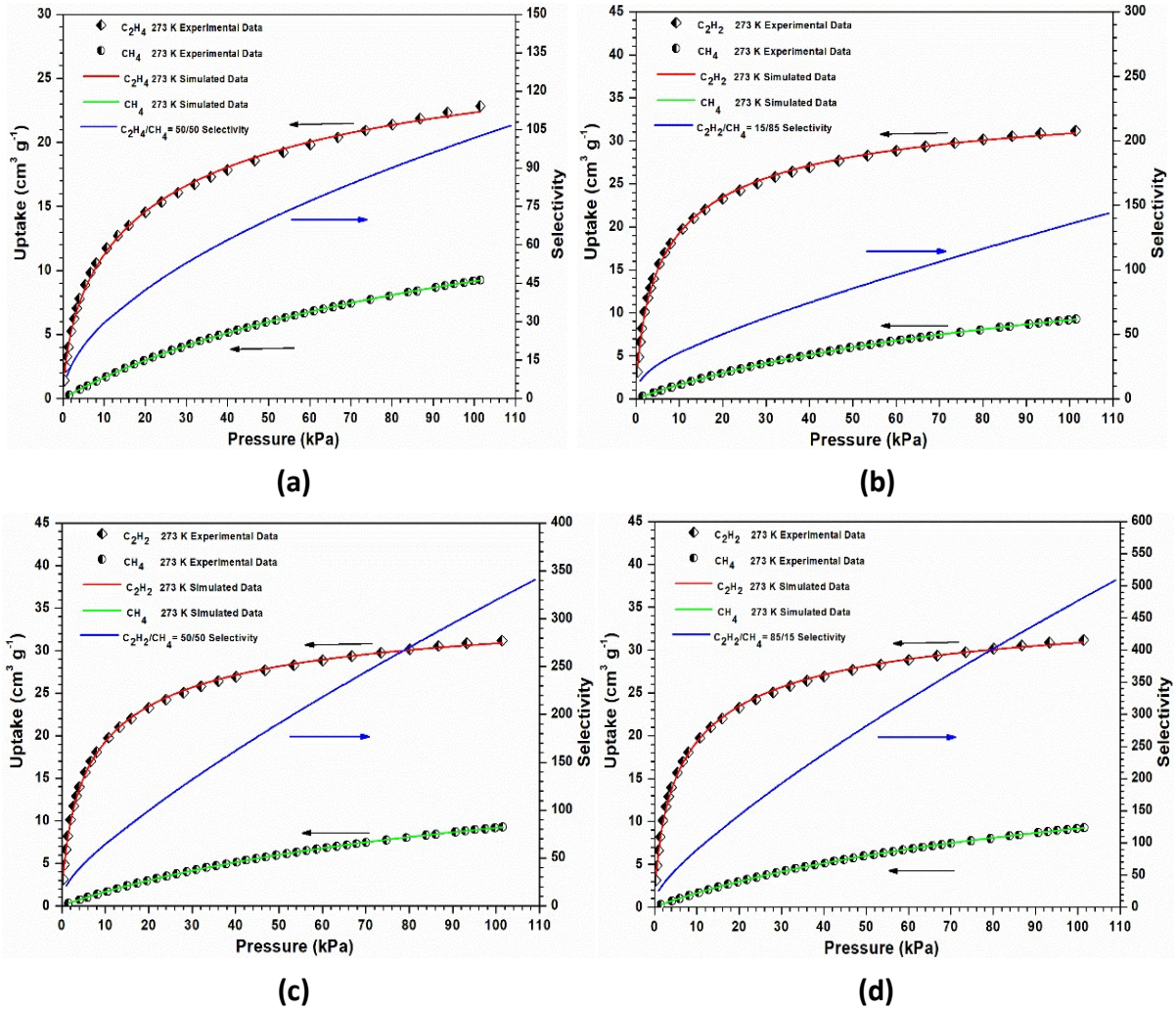

Fig. S10 Comparison of experimental and simulated adsorption isotherms (Left Y axis), and mixture adsorption selectivity predicted by IAST (Right Y axis) of **SNNU-95** for C_2H_4/CH_4 (a, 50-50,) and C_2H_2/CH_4 (b-d: 15-85, 50-50 and 85/15).

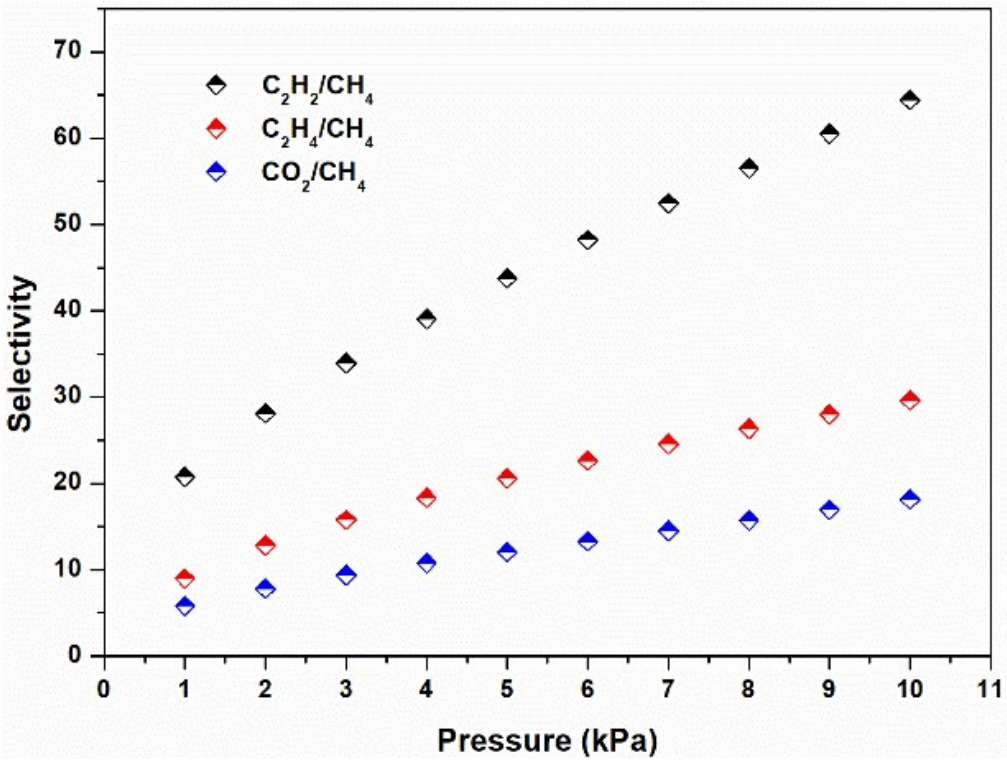

Fig. S11 The comparison of C_2H_2/CH_4, C_2H_4/CH_4 and CO_2/CH_4 selectivity values (50-50) at 273K and low pressure for **SNNU-95**.

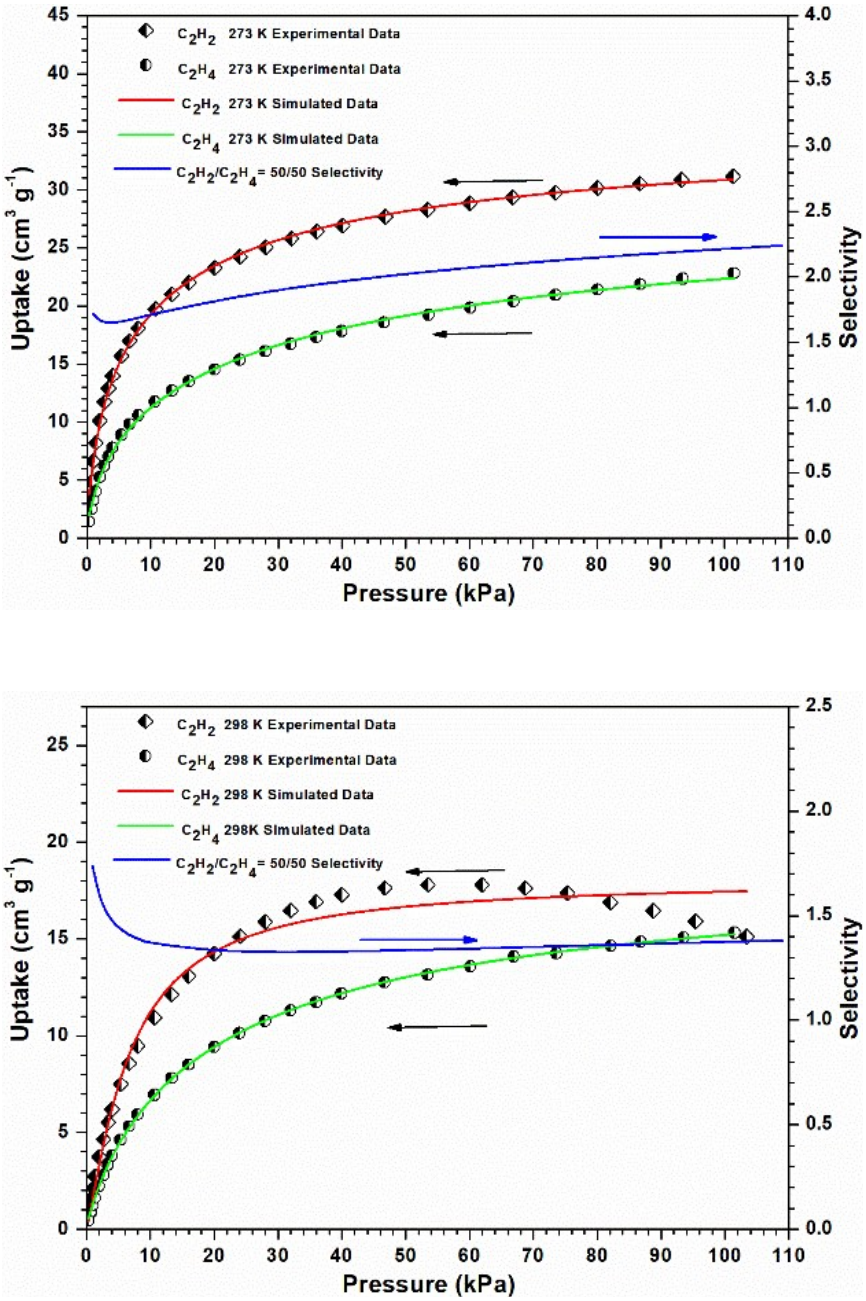

Fig. S12 Comparison of experimental and simulated adsorption isotherms (Left Y axis), and mixture adsorption selectivity predicted by IAST (Right Y axis) of **SNNU-95** for C_2H_2/C_2H_4 (50-50) at different temperatures.

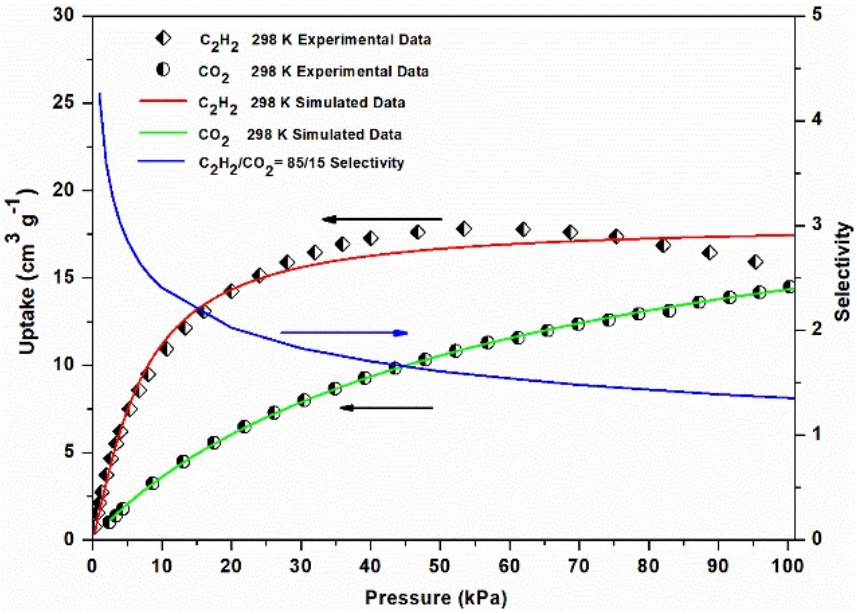

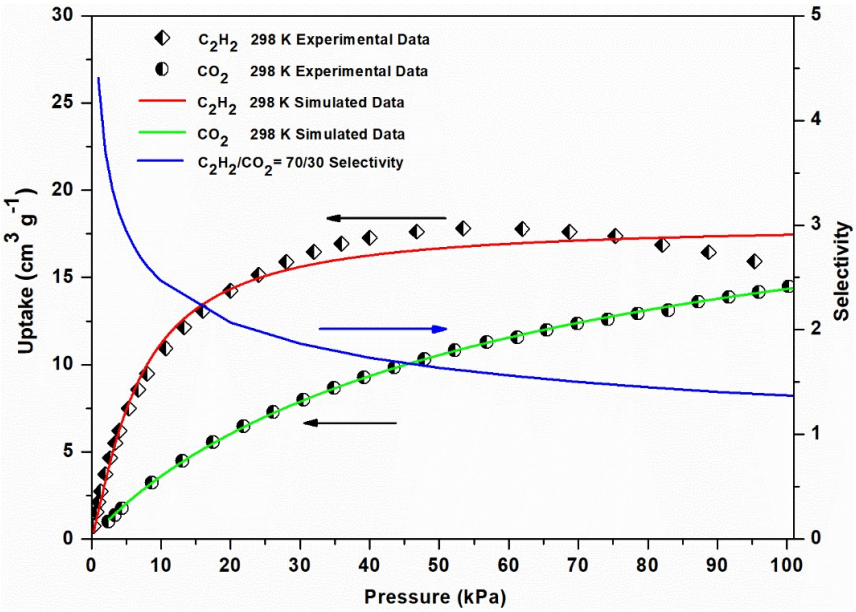

Fig. S13 Comparison of experimental and simulated adsorption isotherms (Left Y axis), and mixture adsorption selectivity predicted by IAST (Right Y axis) of **SNNU-95** for C_2H_2/CO_2 with different ratios.